

International Journal of

STRUCTURAL STABILITY AND DYNAMICS

Volume 2 • Number 2 • June 2002

Editors-in-Chief

Y. B. Yang
C. M. Wang
J. N. Reddy



New Jersey • London • Singapore • Hong Kong • Bangalore

INTERNATIONAL JOURNAL OF STRUCTURAL STABILITY AND DYNAMICS

Editors-in-Chief

Y B Yang Department of Civil Engineering National Taiwan University Taipei, Taiwan 10617 E-mail: ybyang@ce.ntu.edu.tw Tel: 886-2-2363-2104 Fax: 886-2-2363-7585	C M Wang Department of Civil Engineering The National University of Singapore Kent Ridge, Singapore 119260 E-mail: cewcm@nus.edu.sg Tel: 65-874-2157 Fax: 65-779-1635	J N Reddy Department of Mechanical Engineering Texas A&M University College Station, TX 77843-3123, USA E-mail: jnreddy@shakti.tamu.edu Tel: 979-862-2417 Fax: 979-862-3989
---	---	--

International Editorial Board

J F Abel Cornell University, USA	A Eriksson Royal Institute of Technology, Sweden	D A Nethercot Imperial College of Science, Technology and Medicine, UK
Z P Bažant Northwestern University, USA	R P S Han The University of Iowa, USA	J B Obrebski Warsaw University of Technology, Poland
C W Bert The University of Oklahoma, USA	H Irschik Johannes-Kepler University of Linz, Austria	N Ohhoff Aalborg University, Denmark
W F Chen University of Hawaii, USA	W Kanok-Nukulchai Asian Institute of Technology, Thailand	M Papadrakakis National Technical University of Athens, Greece
Y K Cheung University of Hong Kong, Hong Kong	S Kitipornchai City University of Hong Kong, Hong Kong	E Ramm University of Stuttgart, Germany
C K Choi Korea Advanced Institute of Science and Technology, Korea	A W Leissa The Ohio State University, USA	J Rhodes University of Strathclyde, UK
A Combescure LMT-CACHAN, France	A Y T Leung City University of Hong Kong, Hong Kong	N E Shanmugam The National University of Singapore, Singapore
L Corradi Politecnico di Milano, Italy	R Levy Technion-Israel Institute of Technology, Israel	N K Srivastava Université de Moncton, Canada
G De Roeck K U Leuven, Belgium	K M Liew Nanyang Technological University, Singapore	G P Steven The University of Durham, UK
I Elishakoff Florida Atlantic University, USA	C H Loh National Center for Research on Earthquake Engineering, Taiwan	T Tarnai Technical University of Budapest, Hungary
M Eisenberger Technion-Israel Institute of Technology, Israel	Y Q Long Tsinghua University, China	T Usami Nagoya University, Japan
		E Watanabe Kyoto University, Japan

<http://www.worldscientific.com/journals/ijssd/ijssd.html>

International
STRUCTURE
AND

Editors-in-Chief
Y. B. Yang
C. M. Wang
J. N. Reddy

 **World**
New Jersey

STABILITY OF NUMERICAL DISCRETIZATIONS IN MODELLING VIBRATIONAL CHARACTERISTICS OF PIEZOELECTRIC CYLINDRICAL SHELLS

R. V. N. MELNIK

*University of Southern Denmark,
MCI, Mathematical Modelling Group,
Sonderborg, Grundtvigs Alle 150, DK-6400, Denmark
relnik@mci.sdu.dk*

K. N. MELNIK

*Electronic Data Systems – Australia,
60 Currington Street, Sydney, NSW 2000, Australia*

Received 20 July 2001

Accepted 17 May 2002

Many problems in applications of piezoelectric materials are essentially time-dependent, and a conventional treatment of such problems with analytical or semi-analytical techniques based on the analysis of harmonic oscillations become inadequate in those cases where a complete dynamic picture of electromechanical energy transfer is required. For such situations we have developed an efficient explicit numerical methodology allowing us to compute *dynamic* electromechanical characteristics of piezoelectric structures and devices under various loading conditions. In this paper we demonstrate that the stability conditions for our numerical approximation can be obtained from a discrete conservation law, and can be cast in a form similar to that of the classical CFL condition. However, in our case the velocities of wave propagations, participating in the formulation of the stability conditions, are clearly dependent on the pattern of *electromechanical coupling*. Our discussion in this paper, including computational examples, is centred around finite piezoelectric shells of cylindrical shape.

Keywords: Hollow cylindrical shells; piezoelectrics; discrete conservation laws; stability in multiphysics problems.

1. Introduction

With the advances in smart materials and structure technology the role of coupled electromechanical analysis of piezoelectric structures and devices has increased and will continue to do so in a foreseeable future. In many cases we have to deal with intrinsically dynamic processes in this analysis, in which case the solution of the associated problems can be rarely amenable to analytical treatments, and therefore the development of efficient numerical methodologies become an important direction of research in this field.^{1–8}

Since in many cases, including problems in ultrasound applications, structural vibration control, and medical diagnostics, the interest is centered around vibrational characteristics of piezoelectric structures and devices, the analysis of coupled wave dynamics is at the heart of such investigations. When numerical techniques are applied to the solution of such problems the stability of the numerical algorithm becomes one of the major components in the success of the whole mathematical modelling exercise.

In 1928, Courant, Friedrichs and Lewy obtained a fundamental stability condition intrinsic to explicit discretizations of wave dynamics.⁹ They also laid the foundation of what is now known as the energy method. The methodology provides an important tool in constructing conservative numerical schemes for complex problems arising in applied sciences and engineering applications.¹⁰ In this paper we demonstrate how the classical CFL condition can be extended to the case of *coupled dynamics* of electric and mechanical fields. In the 1D case such a generalization of the CFL condition has been already carried out and discussed in detail in Ref. 5, and recently a complete coupling of infinite-length piezoelectric structures with acoustic media has been also considered.⁸ Our main emphasis in this paper is on *finite* piezoelectric shells of cylindrical shape.

We organise this paper as follows.

- In Sec. 2, we provide the reader with the model of coupled dynamic thermopiezoelectricity for cylindrical shells and discuss the importance of accounting for the direction of preliminary polarization in constitutive models when dealing with curvilinear geometry.
- In Sec. 3, we reduce our general model to the case of axisymmetric vibrations of hollow piezoelectric shells, and specify initial and boundary conditions for the problem.
- Sections 4 and 5 give some fundamentals on the well-posedness of the model and the associated conservation laws for fully coupled piezoelectric systems. These considerations are intrinsic to the generalized solution technique on the basis of which the numerical approximation is constructed.
- In Sec. 6, we formulate a discrete conservation law as a tool for a generalization of the CFL stability condition to coupled problems of dynamic piezoelectricity.
- Several illustrative computational results for finite piezoelectric shells of cylindrical shape are given in Sec. 7.

2. Coupled Theory of Piezothermoelectricity for Cylindrical Shells

Piezoelectric rods, beams, and plates have been intensively studied in the literature (e.g. Refs. 11 and 12 and references therein). Curvilinear piezoelectric shells have been studied to a lesser extent since their analysis is a more difficult task,¹³ and in the case where the direction of preliminary polarization is different from the axial (Oz) direction the results are even more sparse. However, for piezoelectric shells

of cylindrical shape preliminary polarizations other than axial become important in many practical applications ranging from piezoelectric gyroscopes, resonators and transducer to structural vibrations of cylindrical shells with sensor/actuator technology. The important point to emphasize in this context is that in such cases constitutive models, coupling mechanical and electric (and, possibly, thermal) fields, are different from those used for the axial preliminary polarization.^{7,14}

Let us consider a general model realizing the coupling between mechanical and electric, and thermal fields based on the system of partial differential equations that consists of equations of motion, the energy balance equation, and the Maxwell equation taken in the dielectric approximation (which is admissible in the acoustic range of frequencies where the Maxwell equation turns into the forced electrostatic equation for dielectrics). The electric field is assumed irrotational, that is $\text{rot}\mathbf{E} = 0$. The system of interest, therefore, has the following form

$$\rho \frac{\partial^2 \mathbf{u}}{\partial t^2} = \nabla \cdot \boldsymbol{\sigma} + \mathbf{F}, \quad T \frac{\partial S}{\partial t} = \text{div} \mathbf{q} + Q, \quad \text{div} \mathbf{D} = G, \quad \mathbf{E} = -\nabla \varphi. \quad (2.1)$$

In the model (2.1), written here in the Cartesian system of coordinates, \mathbf{u} is the displacement vector, ρ is the density of piezoelectric material, $\boldsymbol{\sigma}$ is the stress tensor, S is the system entropy, T is the temperature, \mathbf{q} is the heat flux through the system surface, \mathbf{D} is the electric induction vector, \mathbf{E} is the electric field strength, φ is the electrostatic potential, \mathbf{F} , Q , and G are body (mass) forces on the piezoelectric, the energy due to heat generation inside the body, and the (volume) electric charge density, respectively.

The actual form of the constitutive equations depends on the choice of the thermodynamic potential, which is chosen here in the form of electric enthalpy $H(\epsilon_v, \mathbf{E}, T)$. In this case the stress tensor, $\boldsymbol{\sigma}$, is represented by ($\boldsymbol{\sigma}_v = (\sigma_x, \sigma_y, \sigma_z, \sigma_{yz}, \sigma_{xz}, \sigma_{xy})^T$), and is coupled to the electric and thermal fields via the mechanical strain tensor, $\boldsymbol{\epsilon}$, represented by ($\boldsymbol{\epsilon}_v = (\epsilon_x, \epsilon_y, \epsilon_z, \epsilon_{yz}, \epsilon_{xz}, \epsilon_{xy})^T$)

$$\boldsymbol{\sigma}_v = \mathbf{c} \boldsymbol{\epsilon}_v - \mathbf{e} \mathbf{E} - \gamma T, \quad \mathbf{D} = \boldsymbol{\epsilon} \mathbf{E} + \mathbf{e}^T \boldsymbol{\epsilon}_v + \mathbf{p} T, \quad (2.2)$$

where $\mathbf{c} = (c_{ij})$, $i, j = 1, \dots, 6$ are elastic constants, $\mathbf{e} = (e_{ij})$, $i = 1, 2, 3$, $j = 1, \dots, 6$ are electro-elastic constants (piezomoduli), $\boldsymbol{\epsilon} = (\epsilon_{ij})$, $i, j = 1, 2, 3$ are electric constants (dielectric permittivities), γ gives thermo-elastic constants (the stress temperature coefficients), and \mathbf{p} gives thermo-electric (pyroelectric) constants. In the notation of (2.2), zero-reference temperature is assumed for convenience only (see Ref. 15 for the general case). The relationships between the electric field intensities $\mathbf{E} = (E_x, E_y, E_z)^T$ and the electric potential φ follow from the quasi-static approximation (2.1)

$$E_x = -\frac{\partial \varphi}{\partial x}, \quad E_y = -\frac{\partial \varphi}{\partial y}, \quad E_z = -\frac{\partial \varphi}{\partial z}, \quad (2.3)$$

and the entropy as a function of variables $\boldsymbol{\epsilon}_v$, \mathbf{E} , and T is given as

$$S = \boldsymbol{\gamma}^T \boldsymbol{\epsilon}_v + c_e^V T / T_0 + \mathbf{p}^T \mathbf{E}. \quad (2.4)$$

Materials parameters participating in the formulation of the problems (2.1)–(2.4) depend on the type of non-centrosymmetric crystals chosen (centrosymmetric crystals do not exhibit the piezoeffect). Such crystals are characterized by certain symmetry axes, so that if the internal energy and stresses remain the same under each rotation of the crystal around an axis for the angle $2\pi/n$ we say that the crystal has the n th order symmetry axis. In acousto-electric, acousto-electronic, and acousto-optical applications we deal with piezoelectric materials with anisotropic properties based on crystals of various classes, where the piezoelectric, pyroelectric, and optical properties are subject to non-vanishing the third-rank polar tensor, the polar vector, and the second-rank axial tensor (e.g. Ref. 16). One of the widely used classes in such applications is the orthorhombic class mm2 for which we specify all necessary materials parameters relevant to our further consideration

$$\mathbf{c} = \begin{pmatrix} c_{11} & c_{12} & c_{13} & 0 & 0 & 0 \\ c_{12} & c_{22} & c_{23} & 0 & 0 & 0 \\ c_{13} & c_{23} & c_{33} & 0 & 0 & 0 \\ 0 & 0 & 0 & c_{44} & 0 & 0 \\ 0 & 0 & 0 & 0 & c_{55} & 0 \\ 0 & 0 & 0 & 0 & 0 & c_{66} \end{pmatrix}, \quad \mathbf{e} = \begin{pmatrix} 0 & 0 & e_{31} \\ 0 & 0 & e_{32} \\ 0 & 0 & e_{33} \\ 0 & e_{24} & 0 \\ e_{15} & 0 & 0 \\ 0 & 0 & 0 \end{pmatrix}, \quad (2.5)$$

$$\boldsymbol{\varepsilon} = \begin{pmatrix} \varepsilon_{11} & 0 & 0 \\ 0 & \varepsilon_{22} & 0 \\ 0 & 0 & \varepsilon_{33} \end{pmatrix}, \quad \boldsymbol{\gamma} = (\gamma_{11}, \gamma_{11}, \gamma_{33}, 0, 0, 0)^T, \quad (2.6)$$

$$\mathbf{p} = (0, 0, p_3)^T.$$

This representation is valid for Cartesian coordinates. However, the direct transformation of constitutive Eqs. (2.2) from Cartesian to cylindrical coordinates is possible *only* in the case of the axial preliminary polarization, that is in the case where the axis OZ is chosen in the direction of preliminary polarization. In this case the transformation of coordinates $(x, y, z) \rightarrow (r, \theta, z)$ leads us to the constitutive relationships (2.2) with the same matrices (2.5), (2.6), but in terms of the vectors

$$\boldsymbol{\sigma}_v = (\sigma_r, \sigma_\theta, \sigma_z, \sigma_{\theta z}, \sigma_{rz}, \sigma_{r\theta})^T, \quad \boldsymbol{\epsilon}_v = (\epsilon_r, \epsilon_\theta, \epsilon_z, \epsilon_{\theta z}, \bar{\epsilon}_{rz}, \epsilon_{r\theta})^T, \quad (2.7)$$

$$\mathbf{E}_v = (E_r, E_\theta, E_z)^T, \quad \mathbf{D}_v = (D_r, D_\theta, D_z)^T. \quad (2.8)$$

Even this relatively simple case leads to several additional challenges compared to the case of Cartesian coordinates. The complete set of equations in this case can be written as follows

$$\rho \frac{\partial^2 u_r}{\partial t^2} - \frac{\partial \sigma_{rr}}{\partial r} + \frac{1}{r} \frac{\partial \sigma_{\theta r}}{\partial \theta} + \frac{\partial \sigma_{rz}}{\partial z} + \frac{\sigma_{rr} - \sigma_{\theta \theta}}{r} + F_1, \quad (2.9)$$

$$\rho \frac{\partial^2 u_\theta}{\partial t^2} = \frac{\partial \sigma_{r\theta}}{\partial r} + \frac{1}{r} \frac{\partial \sigma_{\theta \theta}}{\partial \theta} + \frac{\partial \sigma_{\theta z}}{\partial z} + \frac{2\sigma_{r\theta}}{r} + F_2, \quad (2.10)$$

$$\rho \frac{\partial^2 u_z}{\partial t^2} = \frac{\partial \sigma_{rz}}{\partial r} + \frac{1}{r} \frac{\partial \sigma_{\theta z}}{\partial \theta} + \frac{\partial \sigma_{zz}}{\partial z} + \frac{\sigma_{rz}}{r} + F_3, \quad (2.11)$$

$$\frac{1}{r} \frac{\partial D_r}{\partial r} + \frac{1}{r} \frac{\partial D_\theta}{\partial \theta} + \frac{\partial D_z}{\partial z} = G. \quad (2.12)$$

Equations (2.9)–(2.12) remain valid for different types of preliminary polarizations of cylindrical shells. However, as soon as the preliminary polarization of such shells is different from axial, the constitutive relations (2.2) with (2.5), (2.6) cease to become valid, and new relationships should be derived due to the fact that the form of such relationships depends critically on the direction of the vector of preliminary polarization. In particular, for the radial preliminary polarization we introduce new vectors

$$\boldsymbol{\sigma}^r = (\sigma_\theta, \sigma_z, \sigma_r, \sigma_{rz}, \sigma_{r\theta}, \sigma_{\theta z})^T, \quad \boldsymbol{\epsilon}^r = (\epsilon_\theta, \epsilon_z, \epsilon_r, \bar{\epsilon}_{rz}, \epsilon_{r\theta}, \epsilon_{\theta z})^T, \quad (2.13)$$

$$\mathbf{E}^r = (E_\theta, E_z, E_r)^T, \quad \mathbf{D}^r = (D_\theta, D_z, D_r)^T. \quad (2.14)$$

The transformation of coordinates from Cartesian to cylindrical required in this case is $(x, y, z) \rightarrow (\theta, z, r)$. Hence, the constitutive relationships in the case of the radial preliminary polarization of piezoelectric shells take the form

$$\sigma_r = c_{33}\epsilon_r + c_{13}\epsilon_\theta + c_{23}\epsilon_z - e_{33}E_r - \gamma_{33}T, \quad (2.15)$$

$$\sigma_\theta = c_{13}\epsilon_r + c_{11}\epsilon_\theta + c_{12}\epsilon_z - e_{31}E_r - \gamma_{11}T, \quad (2.16)$$

$$\sigma_z = c_{23}\epsilon_r + c_{12}\epsilon_\theta + c_{22}\epsilon_z - e_{32}E_r - \gamma_{22}T, \quad (2.17)$$

$$\sigma_{rz} = c_{44}\bar{\epsilon}_{rz} - e_{24}E_z, \quad \sigma_{r\theta} = c_{55}\epsilon_{r\theta} - e_{15}E_\theta, \quad \sigma_{\theta z} = c_{66}\epsilon_{\theta z}, \quad (2.18)$$

$$D_r = e_{33}\epsilon_r + e_{31}\epsilon_\theta + e_{32}\epsilon_z + \varepsilon_{33}E_r + p_3T, \quad (2.19)$$

$$D_\theta = e_{15}\epsilon_{r\theta} + \varepsilon_{11}E_\theta, \quad D_z = e_{24}\epsilon_{rz} + \varepsilon_{22}E_z. \quad (2.20)$$

The above relationships are simplified if the crystal posses some additional symmetry. For example, for the hexagonal class 6mm the elastoelectric properties of the crystals are invariant for any rotation about the principal axis (in the Cartesian coordinates), so that such piezoelectric crystals are transversely isotropic (the crystal of this class has a six-fold symmetry axis parallel to Oz). Note that in piezoelectric ceramics the transverse isotropy is perpendicular to the direction of polarization, and this is the reason why we can characterize elastic, electric, piezoelectric properties of piezoceramics by tensors in the same form as those for class 6mm (e.g. Ref. 17, Vol. 1, p. 161). The simplifications for the class 6mm are summarized by the following relationships

$$c_{55} = c_{44}, c_{66} = \frac{1}{2}(c_{11} - c_{12}), c_{22} = c_{11}, c_{23} = c_{13}, e_{24} = e_{15}, \epsilon_{22} = \epsilon_{11}, \gamma_{22} = \gamma_{11}. \quad (2.21)$$

Our comment made about the mm2 class remains in place for this class as well. The fact that the actual form of the constitutive relationships for cylindrical piezoelectrics of class 6mm, coupling together mechanical, electric, and thermal fields, depends on the type of the preliminary polarization is worthwhile to emphasize again, especially in the context of piezoelectric ceramics applications. Since we deal with macroscopic piezoelectric responses, it is important to realize that we have to induce a preferred direction of polarization within a piezoelectric component. Moreover, with further advances in sensor/actuator design and other applications of piezoelectric ceramics, this issue cannot be overlooked because, after all, piezoelectric ceramics is a polycrystalline structure whose dielectric properties are inherently nonlinear due to, amongst other things, a nonlinear polarization-electric field dependency.

Depending on a specific situation, additional assumptions are needed to connect strains and displacements. For example, nonlinear effects might become important for piezoelectric systems exposed to large thermal gradients, as well as for flexible piezoelectric-based structures subjected to dynamic excitations. In the later case, geometric nonlinearities of the system and possibilities of large deformations make linear models inadequate. In such cases one of several well-known approximations of shell dynamics can be incorporated into the model for the piezoelectric system. If, for example, the shell has the structure similar to that of an acoustic cavity but with a relatively short length compared to its diameter, one can base the derivation of the governing equations on the Donnell–Mushtari–Vlasov model. However, when the length of the shell is comparable to its diameter, higher order theories such as Byrne–Flugge–Lur’ye should be used (e.g. Ref. 18 and references therein). We note also that it is often possible to assume that nonlinear deflections in one of the coordinate directions is much more prominent compared to the other two. For example, for thin circular plates the von Karman type assumption is often used to simplify the problem by considering the transverse nonlinear deflections as dominant compared to the other two (in-plane) deflections, so that the nonlinear effects in the in-plane deflections are neglected. This assumption, combined with the Kirchhoff–Love assumption (the displacements vary linearly through the shell thickness in the Oz-direction), is used frequently for thin circular discs/plates allowing to obtain the relationships between the “membrane”, ϵ_{ij}^m , and “bending” strains, ϵ_{ij}^b , and displacements, which, e.g. for circular thin plates we have the following form of these relationships (e.g. Ref. 19 and references therein)

$$\epsilon_r^m = \frac{\partial u_r}{\partial r} + \frac{1}{2} \left(\frac{\partial u_z}{\partial r} \right)^2, \quad \epsilon_\theta^m = \frac{u_r}{r} + \frac{1}{r} \frac{\partial u_\theta}{\partial \theta} + \frac{1}{2} \left(\frac{1}{r} \frac{\partial u_z}{\partial \theta} \right)^2, \quad (2.22)$$

$$\epsilon_{r\theta}^m = \frac{\partial u_\theta}{\partial r} + \frac{1}{r} \frac{\partial u_r}{\partial \theta} + \left(\frac{1}{r} \frac{\partial u_z}{\partial r} \frac{\partial u_z}{\partial \theta} \right), \quad \epsilon_r^b = -\frac{\partial^2 u_z}{\partial r^2}, \quad (2.23)$$

$$\epsilon_\theta^b = - \left(\frac{1}{r} \frac{\partial u_z}{\partial r} + \frac{1}{r^2} \frac{\partial^2 u_z}{\partial \theta^2} \right), \quad \epsilon_{r\theta}^b = -2 \frac{\partial}{\partial r} \left(\frac{1}{r} \frac{\partial u_z}{\partial \theta} \right). \quad (2.24)$$

Then, the total strain is split into two parts, due to the membrane forces, and due to bending moments, both dependent on elastic, electric, and thermal effects

$$\begin{Bmatrix} \epsilon_r \\ \epsilon_\theta \\ \epsilon_{r\theta} \end{Bmatrix} = \begin{Bmatrix} \epsilon_r^m \\ \epsilon_\theta^m \\ \epsilon_{r\theta}^m \end{Bmatrix} + z \begin{Bmatrix} \epsilon_r^b \\ \epsilon_\theta^b \\ \epsilon_{r\theta}^b \end{Bmatrix}, \quad (2.25)$$

where z expresses the linear variation in the Oz-direction according to the Kirchhoff–Love hypothesis.

These expressions can be used in constitutive Eqs. (2.2) for cylindrical piezoelectric systems, and if such a system is made of piezoceramics, the resulting constitutive model will coincide with the state equations for piezoelectric crystals of class 6mm with the symmetry axis Oz (see (2.7), (2.8), (2.21)) only in the case of the axial preliminary polarization. Indeed, only in the case where the external field of preliminary polarization has some symmetry properties it is possible to use constitutive equations with constant coefficients in cylindrical system of coordinates since in the general case the direction of the external electric field of preliminary polarization is not homogeneous, and may change inside of the volume of the piezoelectric. In the case of the radial preliminary polarization the constitutive models (2.15)–(2.20) should be used.

In what follows we focus on the stability issues of discretized models, and we set outside the scope of this paper thermal and nonlinear effects which have been initially studied in Ref. 15. In this case the strain-displacements relationships can be written in the Cauchy form

$$\epsilon_r = \frac{\partial u_r}{\partial r}, \quad \epsilon_\theta = \frac{1}{r} \frac{\partial u_\theta}{\partial \theta} + \frac{u_r}{r}, \quad \epsilon_z = \frac{\partial u_z}{\partial z}, \quad (2.26)$$

$$\epsilon_{\theta z} = \frac{\partial u_\theta}{\partial z} + \frac{1}{r} \partial u_z \partial \theta, \quad \bar{\epsilon}_{rz} = \frac{\partial u_r}{\partial z} + \frac{\partial u_z}{\partial r}, \quad \epsilon_{r\theta} = \frac{1}{r} \frac{\partial u_r}{\partial \theta} + \frac{\partial u_\theta}{\partial r} - \frac{u_\theta}{r}. \quad (2.27)$$

In the next section we reduce the model discussed here to the case of axisymmetric vibrations, for which we use the following notation $\epsilon_{rz} = \frac{1}{2} \bar{\epsilon}_{rz}$.

3. Axisymmetric Vibrations of Hollow Piezoelectric Shells

In this case the system considered in the previous section is simplified to take the following form:

$$\rho \frac{\partial^2 u_r}{\partial t^2} = \frac{\partial \sigma_r}{\partial r} + \frac{\partial \sigma_{rz}}{\partial z} + \frac{\sigma_r - \sigma_\theta}{r} + f_1, \quad \rho \frac{\partial^2 u_z}{\partial t^2} = \frac{\partial \sigma_{rz}}{\partial r} + \frac{\partial \sigma_z}{\partial z} + \frac{\sigma_{rz}}{r} + f_2, \quad (3.1)$$

$$\frac{1}{r} \frac{\partial}{\partial r} (r D_r) + \frac{\partial D_z}{\partial z} = f_3, \quad (3.2)$$

Models (3.1)–(3.2) is considered in the space-time region

$$\bar{Q}_T = \bar{G} \times \bar{I}, \quad \bar{G} = \{(r, z) : R_0 \leq r \leq R_1, Z_0 \leq z \leq Z_1\}, \quad \bar{I} = \{t : 0 \leq t \leq T\}, \quad (3.3)$$

meaning that we deal with the shells of hollow cylindrical geometry such as those depicted in Fig. 1. Structures and devices of this geometrical configuration are important in many applications and have a long history of research in the context of conventional elasticity with the interest fueled by the importance of the associated problems even in much simplified settings (e.g. Ref 20, Sec. 12). In the context of smart material and structure technology with embedded sensors/actuators based on piezoelectrics the importance of these problems will continue to increase.

For cylindrical shells preliminary polarized radially (see Fig. 1) the state equations for piezoceramics read

$$\sigma_r = c_{33}\epsilon_r + c_{13}(\epsilon_\theta + \epsilon_z) - e_{33}E_r, \quad \sigma_\theta = c_{13}\epsilon_r + c_{11}\epsilon_\theta + c_{12}\epsilon_z - e_{13}E_r, \quad (3.4)$$

$$\sigma_z = c_{13}\epsilon_r + c_{12}\epsilon_\theta + c_{11}\epsilon_z - e_{13}E_r, \quad \sigma_{rz} = c_{44}\epsilon_{rz} - e_{15}E_z, \quad (3.5)$$

$$D_r = e_{33}\epsilon_r + e_{13}(\epsilon_\theta + \epsilon_z) + \epsilon_{33}E_r, \quad D_z = 2e_{15}\epsilon_{rz} + \epsilon_{11}E_z. \quad (3.6)$$

The condition of non-negativity of the potential energy of deformation,

$$\delta_1 \sum_{i=1}^4 \xi_i^2 \leq c_{33}\xi_1^2 + c_{11}(\xi_2^2 + \xi_3^2) + 2c_{13}(\xi_2\xi_1 + \xi_3\xi_1) + 2c_{12}\xi_3\xi_2 + 2c_{44}\xi_4^2, \quad \delta_1 > 0, \quad (3.7)$$

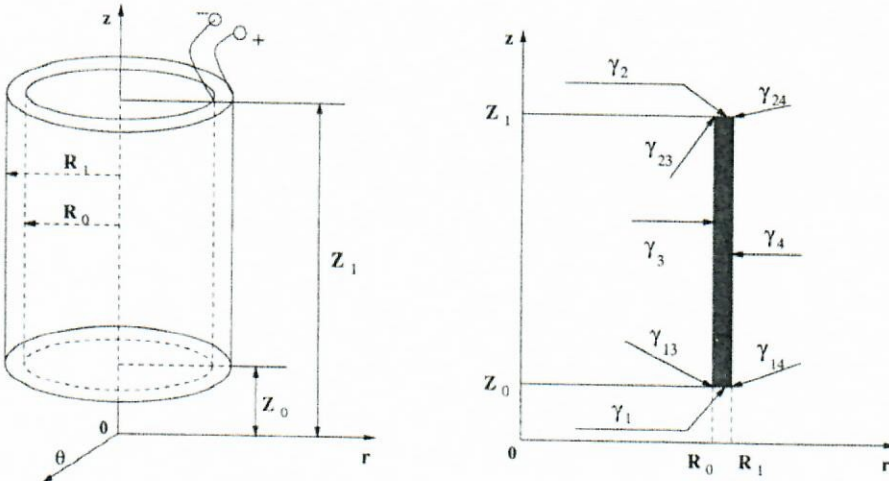


Fig. 1. Geometry and boundary condition specifications for the problem of interest.

is assumed, and given functions $u_r^{(i)}$ and $u_z^{(i)}$, $i = 0, 1$ the model (3.1)–(3.7) is supplemented by the initial conditions

$$u_r(r, z, 0) = u_r^{(0)}(r, z), \quad \frac{\partial u_r(r, z, 0)}{\partial t} = u_r^{(1)}(r, z), \quad (3.8)$$

$$u_z(r, z, 0) = u_z^{(0)}(r, z), \quad \frac{\partial u_z(r, z, 0)}{\partial t} = u_z^{(1)}(r, z). \quad (3.9)$$

For mechanical boundary conditions we have chosen

$$\sigma_r(R_i, z, t) = p_r^{(i)}(z, t), \quad \sigma_z(r, Z_i, t) = p_z^{(i)}(r, t), \quad (3.10)$$

$$\sigma_{rz}(R_i, z, t) = p_{zt}^{(i)}(z, t), \quad \sigma_{rz}(r, Z_i, t) = p_{rt}^{(i)}(r, t), \quad (3.11)$$

where $p_r^{(i)}$, $p_z^{(i)}$, $p_{zt}^{(i)}$, $p_{rt}^{(i)}$ ($i = 0, 1$) are given functions. This is the most challenging case since the mechanical and electric fields become coupled on the boundaries of the shell in addition to the conventional coupling via Eqs. (3.1) and (3.2). Other possible mechanical boundaries, e.g. where u_r and u_z are given on the external boundary can be treated as a special case of (3.10)–(3.11). Note also that ideal mechanical (and electrical) matching conditions (continuity conditions across the internal boundary) may be imposed as well instead of the internal boundary conditions considered in (3.10)–(3.11) for $i = 0$. Such a consideration, which is typical for fluid-structure interaction problems,⁸ can be also treated as a special case of our formulation. Electrical boundary conditions are taken here in the form

$$\varphi(R_i, z, t) = 0, \quad D_z(r, Z_i, t) = 0, \quad i = 0, 1. \quad (3.12)$$

The choice of electrical boundary conditions depends on the way how the electric energy is supplied to the piezoelectric system or device of interest. In the case considered here it is assumed that the external and internal (circular) surfaces are fully covered by electrodes (the first condition), and that the cylinder base surfaces are free of electrodes (the second condition). The dielectric permittivity of the surrounding media is assumed to be much less than the dielectric permittivity of piezoceramics which is true for vacuum and air. Other electric conditions can be formulated in a similar way, e.g. where the cylinder is only partially covered by electrodes, and/or on the internal surface we have continuity conditions for φ and D_r , etc. Of course, these different conditions result in different outcomes when solving realistic problems. For example, characteristics of piezoelectric elements such as the electromechanical coupling coefficient are dependent on the position and size of the electrodes.²¹ However, all such cases can be treated within the general framework proposed here. Note also that the homogeneity of the electrical conditions (3.12) does not restrict the generality of the model since problems with nonhomogeneous conditions can be reduced to the homogeneous case by the known procedure.⁵ In the case considered here the electric field representation in terms of

the electrostatic potential, and the Cauchy relationships considered in the previous section are simplified to

$$\begin{aligned} E_r &= -\frac{\partial \varphi}{\partial r}, & E_z &= -\frac{\partial \varphi}{\partial z}, & \epsilon_r &= \frac{\partial u_r}{\partial r}, & \epsilon_\theta &= \frac{u_r}{r}, \\ \epsilon_z &= \frac{\partial u_z}{\partial z}, & \epsilon_{rz} &= \frac{1}{2} \left(\frac{\partial u_r}{\partial z} + \frac{\partial u_z}{\partial r} \right). \end{aligned} \quad (3.13)$$

Now we are in a position to characterize model (3.1)–(3.13) by the associated conservation law.

4. Evolution of Energy and Conservation Laws for Fully Coupled Piezoelectric Systems

In many engineering applications solutions to problems described by models (3.1)–(3.13) might not be smooth in the classical sense. For example, typical piezoelectric transducers can operate in a piston-like mode indicating steep gradients in radial displacements. In a series of previous papers a general methodology for the construction of numerical schemes for the solution of fully coupled problems of piezoelectricity accounting for such situations has been proposed and rigorously justified.^{5–7} The coupled system of *dynamic* piezoelectricity originated from fundamental works by W. Voigt²² and developed by many other researchers has been shown to be mathematically well-posed for the first time in 1988 by the first author (see Ref. 23 and references therein) where the regularity of the solution has been investigated in detail.

The basic idea of the discussion that follows in this paper stems from the general conservation law describing the dynamics of the internal energy of the coupled electromechanical system. Recall that the internal energy of the system described by models (3.1)–(3.13) can be represented in the following form (e.g. Ref. 7)

$$\begin{aligned} \mathcal{E} = & \frac{\rho}{2} \int \int_{\Omega} r \left\{ \left(\frac{\partial u_r}{\partial t} \right)^2 + \left(\frac{\partial u_z}{\partial t} \right)^2 \right\} d\Omega \\ & + \frac{1}{2} \int \int_{\Omega} r \{ c_{33} \epsilon_r^2 + c_{11} (\epsilon_\theta^2 + \epsilon_z^2) + 2c_{13} (\epsilon_\theta \epsilon_r + \epsilon_z \epsilon_r) + 2c_{12} \epsilon_z \epsilon_\theta + 2c_{44} \epsilon_{rz}^2 \} d\Omega \\ & + \frac{\epsilon_{33}}{2} \int \int_{\Omega} r E_r^2 d\Omega + \frac{\epsilon_{11}}{2} \int \int_{\Omega} r E_z^2 d\Omega. \end{aligned} \quad (4.1)$$

Three lines in (4.1) represent the kinetic energy of the system, the energy of elastic deformations, and the energy of the electric field, respectively. It can be shown (see Ref. 7) that the functional defined by (4.1) is bounded. An *a priori* estimate for the solution of (3.1)–(3.13), derived in terms of the initial data of the model, is based on the energy balance equation which can be written in the following form⁷

$$\frac{d\mathcal{E}}{dt} = \int \int_{\Omega} r \left[\frac{\partial D_r}{\partial t} E_r + \frac{\partial D_z}{\partial t} E_z \right] d\Omega + \int_{R_0}^{R_1} r \left[\sigma_{rz} \frac{\partial u_r}{\partial t} + \sigma_z \frac{\partial u_z}{\partial t} \right] dr \Big|_{Z_0}^{Z_1}$$

$$+ \int_{Z_0}^{Z_1} r \left[\sigma_r \frac{\partial u_r}{\partial t} + \sigma_{rz} \frac{\partial u_z}{\partial t} \right] dz \Big|_{R_0}^{R_1} + \iint_{\Omega} r \left[f_1 \frac{\partial u_r}{\partial t} + f_2 \frac{\partial u_z}{\partial t} \right] d\Omega. \quad (4.2)$$

The conservation law (4.2) is the foundation upon which the subsequent numerical approximation is built. Moreover, it will be shown that the discrete analogue of (4.2) will lead to the stability condition of such an approximation.

5. Numerical Discretizations Based on Variational Difference Schemes

One of the most fundamental contributions to the field of numerical analysis, as well as to the related fields of partial differential equations and engineering mathematics, is the development of the general methodology for constructing numerical schemes based on the energy method. Although the method can be traced back to early works by Courant and co-authors,⁹ its wide spread applications began several decades later. With a number of practical examples leading to discontinuous solutions of PDE-based models, it has been realized that physical processes and phenomena can be effectively characterized by some conservation laws, and therefore it is natural to attempt to preserve properties of the system governing by such laws when numerical approximations are constructed. Several efficient methodologies exist now for the construction of such *conservative* approximations,¹⁰ one of which, essentially developed from the energy method,⁷ was used to construct a numerical scheme for the solution of (3.1)–(3.13).

We remark that the claim that the energy method “was primarily studied to prove the stability, existence, and uniqueness of solutions of schemes” and “the main emphasis was on stability rather than conservation property” expressed recently by several authors on this new wave of interest to the energy method (e.g. Ref. 24) is only partly true. Indeed, the methodology has been used widely for *the construction of conservative numerical schemes*, and it has been extensively developed for several decades (e.g. Ref. 10 and 25). However, it is certainly true that *the constructive procedure for deriving conservative numerical schemes allows us to obtain stability conditions for the resulting discretizations*. It is our aim in this paper to demonstrate that the classical CFL stability condition originated from Ref. 9 can be generalized to the model of piezoelectricity via the energy method. The resulting conditions have a clear physical meaning, and we explain this in detail in the remainder of this paper. One final remark, before proceeding with the discretization of (3.1)–(3.13), goes to the fact that the idea, and its subsequent success in such constructions, can often be attributed to some invariance properties of the original PDE-based model which lead to the possibility of applying Noether’s theorem to obtain conservation laws. A further development of this idea, closely linked to transformations of solutions of differential equations, leads to an increasing interest

to the Lie group approach to differential models and the associated methodology of geometric integration (e.g. Ref. 26 and 27 and references therein).

The procedure of the construction of numerical approximation to (3.1)–(3.13) was explained in detail in Ref. 7, and here we remind only the result of that construction. We use the following notation from theory of difference schemes (e.g. Refs. 10 and 24)

$$\delta_+^x u(x, t) = \frac{u(x + \Delta x, t) - u(x, t)}{\Delta x}, \quad \delta_-^x u(x, t) = \frac{u(x, t) - u(x - \Delta x, t)}{\Delta x}, \quad (5.1)$$

$$\delta_x^2 u(x, t) = (u(x + \Delta x, t) - 2u(x, t) + u(x - \Delta x, t)) / (\Delta x)^2. \quad (5.2)$$

In the case of higher dimensions considered here we use analogous notation with changing subindex x for the appropriate spatial coordinate (e.g. r or z in our case of cylindrical coordinates). When appropriate, we use the same notation for time difference derivatives by changing the subindex to t .

The space-time region of the problem \bar{Q}_T is covered by a grid $\bar{\omega}_{h\tau} = \bar{\omega}_h \times \bar{\omega}_\tau$, where $\bar{\omega}_h = \bar{\omega}_{h_1} \times \bar{\omega}_{h_2}$ is the spatial grid with $\bar{\omega}_{h_1} = \{r_i : r_i = R_0 + ih_1, i = 0, 1, \dots, N, h_1 = (R_1 - R_0)/N\}$, $\bar{\omega}_{h_2} = \{z_j : z_j = Z_0 + jh_2, j = 0, 1, \dots, M, h_2 = (Z_1 - Z_0)/M\}$, and $\bar{\omega}_\tau = \{t_k : t_k = k\tau, \tau = T/L, k = 0, 1, \dots, L\}$ is the temporal grid. The overbar over nodes like $\bar{r} = r - h_1/2$, $\bar{z} = z - h_2/2$ denotes “flux” nodes where values of deformations and stresses will be computed. On several occasions we will need auxiliary spatial grids in the r -direction, e.g. $\omega_{h_1} = \{r_i = R_0 + ih_1, i = 1, \dots, N-1\}$, $\omega_{h_1}^+ = \{r_i = R_0 + ih_1, i = 1, \dots, N\}$, $\omega_{h_1}^- = \{r_i = R_0 + ih_1, i = 0, \dots, N-1\}$ (in a similar way we define auxiliary spatial grids in the z -direction $\omega_{h_2}, \omega_{h_2}^+, \omega_{h_2}^-$). As it is seen from Fig. 1, we define the boundary of the spatial region G as $\gamma_1 = \{(r, z) : R_0 < r < R_1, z = Z_0\}$, $\gamma_2 = \{(r, z) : R_0 < r < R_1, z = Z_1\}$, $\gamma_3 = \{(r, z) : r = R_0, Z_0 < z < Z_1\}$, $\gamma_4 = \{(r, z) : r = R_1, Z_0 < z < Z_1\}$, with $\gamma_{13} = \{r = R_0, z = Z_0\}$, $\gamma_{23} = \{r = R_0, z = Z_1\}$, $\gamma_{24} = \{r = R_1, z = Z_1\}$, and $\gamma_{14} = \{r = R_1, z = Z_0\}$ being the corner points of this region. Finally, $\hat{y} \equiv y(r, z, t + \tau)$ will denote the discrete function y from the “upper” time layer, while its counterpart from the “lower” time layer will be denoted by $\check{y} \equiv y(r, z, t - \tau)$. If the time layer index is omitted, it is assumed that the value is taken from the current time layer t . Then, the numerical approximation we are interested in can be written as follows

$$\rho \delta_t^2 y = \Lambda_1(y, g, \mu) + F_1, \quad \rho \delta_t^2 g = \Lambda_2(y, g, \mu) + F_2, \quad \Lambda_3(y, g, \mu) = F_3, \quad (5.3)$$

where functions y, g and μ are discrete-argument functions that give approximations to the functions $u_r(r, z, t), u_z(r, z, t)$ and $\varphi(r, z, t)$ respectively. These functions are taken at time n when values of the difference operators $\Lambda_i, i = 1, 2, 3$ are computed. These operators and the right hand sides $F_i, i = 1, 2, 3$ in (3.5) are defined as follow (see Fig. 1):

- For $(r, z) \in \omega_h$

$$\Lambda_1(y, g, \mu) = \frac{1}{r} \delta_+^r \left(\bar{r} \frac{\bar{\sigma}_r + \bar{\sigma}_r^{+1z}}{2} \right) + \frac{1}{r} \delta_+^z (\bar{r} \bar{\sigma}_{rz} + \bar{r}^{(+1)} \bar{\sigma}_{rz}^{(+1r)})$$

$$- \frac{\bar{\sigma}_\theta + \bar{\sigma}_\theta^{(+1r)} + \bar{\sigma}_\theta^{(+1z)} + \bar{\sigma}_\theta^{(+1,+1)}}{4r},$$

$$\Lambda_2(y, g, \mu) = \frac{1}{r} \delta_+^r \left(\bar{r} \frac{\bar{\sigma}_{rz} + \bar{\sigma}_{rz}^{+1z}}{2} \right) + \frac{1}{r} \delta_+^z (\bar{r} \bar{\sigma}_z + \bar{r}^{(+1)} \bar{\sigma}_z^{(+1r)}),$$

$$\Lambda_3(y, g, \mu) = \frac{1}{r} \delta_+^r \left(\bar{r} \frac{\bar{D}_r + \bar{D}_r^{+1z}}{2} \right) + \frac{1}{r} \delta_+^z (\bar{r} \bar{D}_z + \bar{r}^{(+1)} \bar{D}_z^{(+1r)}),$$

$$F_1 = f_1, \quad F_2 = f_2, \quad F_3 = f_3.$$

- For $(r, z) \in \gamma_1$

$$\Lambda_1 = \frac{1}{r} \delta_+^r (\bar{r} \bar{\sigma}_r^{(+1z)}) + \frac{1}{r} \frac{2}{h_2} \left(\frac{\bar{r} \bar{\sigma}_{rz}^{(+1z)} + \bar{r}^{(+1)} \bar{\sigma}_{rz}^{(+1,+1)}}{2} \right) - \frac{\bar{\sigma}_\theta^{(+1z)} + \bar{\sigma}_\theta^{(+1,+1)}}{2r},$$

$$\Lambda_2 = \frac{1}{r} \delta_+^r (\bar{r} \bar{\sigma}_{rz}^{(+1z)}) + \frac{1}{r} \frac{2}{h_2} \left(\frac{\bar{r} \bar{\sigma}_z^{(+1z)} + \bar{r}^{(+1)} \bar{\sigma}_z^{(+1,+1)}}{2} \right),$$

$$\Lambda_3 = \frac{1}{r} \delta_+^r (\bar{r} \bar{D}_r^{(+1z)}) + \frac{1}{r} \frac{2}{h_2} \left(\frac{\bar{r} \bar{D}_z^{(+1z)} + \bar{r}^{(+1)} \bar{D}_z^{(+1,+1)}}{2} \right),$$

$$F_1 = f_1 - \frac{2}{h_2} p_{rt}^{(0)}, \quad F_2 = f_2 - \frac{2}{h_2} p_z^{(0)}, \quad F_3 = f_3.$$

- For $(r, z) \in \gamma_2$

$$\Lambda_1 = \frac{1}{r} \delta_+^r (\bar{r} \bar{\sigma}_r) - \frac{1}{r} \frac{2}{h_2} \left(\frac{\bar{r} \bar{\sigma}_{rz} + \bar{r}^{(+1)} \bar{\sigma}_{rz}^{(+1r)}}{2} \right) - \frac{\bar{\sigma}_\theta + \bar{\sigma}_\theta^{(+1r)}}{2r},$$

$$\Lambda_2 = \frac{1}{r} \delta_+^r (\bar{r} \bar{\sigma}_{rz}) - \frac{1}{r} \frac{2}{h_2} \left(\frac{\bar{r} \bar{\sigma}_z + \bar{r}^{(+1)} \bar{\sigma}_z^{(+1r)}}{2} \right) - \frac{\bar{\sigma}_\theta + \bar{\sigma}_\theta^{(+1r)}}{2r},$$

$$\Lambda_3 = \frac{1}{r} \delta_+^r (\bar{r} \bar{D}_r) - \frac{1}{r} \frac{2}{h_2} \left(\frac{\bar{r} \bar{D}_z + \bar{r}^{(+1)} \bar{D}_z^{(+1r)}}{2} \right),$$

$$F_1 = f_1 + \frac{2}{h_2} p_{rt}^{(1)}, \quad F_2 = f_2 + \frac{2}{h_2} p_z^{(1)}, \quad (r, z) \in \gamma_2, \quad F_3 = f_3.$$

- For $(r, z) \in \gamma_3$

$$\Lambda_1 = \frac{1}{r} \bar{r}^{(+1)} \delta_+^z (\bar{\sigma}_{rz}^{(+1r)}) + \frac{1}{r} \frac{2}{h_1} \bar{r}^{(+1)} \left(\frac{\bar{\sigma}_r^{(+1r)} + \bar{\sigma}_r^{(+1,+1)}}{2} \right) - \frac{\bar{\sigma}_\theta^{(+1r)} + \bar{\sigma}_\theta^{(+1,+1)}}{2r},$$

$$\Lambda_2 = \frac{1}{r} \bar{r}^{(+1)} \delta_+^z (\bar{\sigma}_z^{(+1_r)}) + \frac{1}{r} \frac{2}{h_1} \bar{r}^{(+1)} \left(\frac{\bar{\sigma}_{rz}^{(+1_r)} + \bar{\sigma}_{rz}^{(+1,+1)}}{2} \right),$$

$$\Lambda_3 = \mu, \quad F_1 = f_1 - \frac{2}{h_1} p_r^{(0)}, \quad F_2 = f_2 - \frac{2}{h_1} p_{zt}^{(0)}, \quad F_3 = 0.$$

- For $(r, z) \in \gamma_4$

$$\Lambda_1 = \frac{1}{r} \bar{r} \delta_+^z (\bar{\sigma}_{rz}) - \frac{1}{r} \frac{2}{h_1} \bar{r} \left(\frac{\bar{\sigma}_r + \bar{\sigma}_r^{(+1_z)}}{2} \right) - \frac{\bar{\sigma}_\theta + \bar{\sigma}_\theta^{(+1_z)}}{2r},$$

$$\Lambda_2 = \frac{1}{r} \bar{r} \delta_+^z (\bar{\sigma}_z) - \frac{1}{r} \frac{2}{h_1} \bar{r} \left(\frac{\bar{\sigma}_{rz} + \bar{\sigma}_{rz}^{(+1_z)}}{2} \right),$$

$$\Lambda_3 = \mu, \quad F_1 = f_1 + \frac{2}{h_1} p_{rt}^{(1)}, \quad F_2 = f_2 + \frac{2}{h_1} p_{zt}^{(1)}, \quad F_3 = 0.$$

- For $(r, z) \in \gamma_{13}$

$$\Lambda_1 = \frac{1}{r} \frac{2}{h_1} \bar{r}^{(+1)} \bar{\sigma}_r^{(+1,+1)} + \frac{1}{r} \frac{2}{h_2} \bar{r}^{(+1)} \bar{\sigma}_{rz}^{(+1,+1)} - \frac{\bar{\sigma}_\theta^{(+1,+1)}}{r},$$

$$\Lambda_2 = \frac{1}{r} \frac{2}{h_2} \bar{r}^{(+1)} \bar{\sigma}_z^{(+1,+1)} + \frac{1}{r} \frac{2}{h_1} \bar{r}^{(+1)} \bar{\sigma}_{rz}^{(+1,+1)},$$

$$\Lambda_3 = \mu, \quad F_1 = f_1 - \frac{2}{h_1} p_r^{(0)} - \frac{2}{h_2} p_{rt}^{(0)}, \quad F_2 = f_2 - \frac{2}{h_1} p_{zt}^{(0)} - \frac{2}{h_2} p_z^{(0)}, \quad F_3 = 0.$$

- For $(r, z) \in \gamma_{23}$

$$\Lambda_1 = \frac{1}{r} \frac{2}{h_1} \bar{r}^{(+1)} \bar{\sigma}_r^{(+1_r)} - \frac{1}{r} \frac{2}{h_2} \bar{r}^{(+1)} \bar{\sigma}_{rz}^{(+1_r)} - \frac{\bar{\sigma}_\theta^{(+1_r)}}{r},$$

$$\Lambda_2 = \frac{1}{r} \frac{2}{h_1} \bar{r}^{(+1)} \bar{\sigma}_{rz}^{(+1_r)} - \frac{1}{r} \frac{2}{h_2} \bar{r}^{(+1)} \bar{\sigma}_z^{(+1_r)},$$

$$\Lambda_3 = \mu, \quad F_1 = f_1 - \frac{2}{h_1} p_r^{(0)} + \frac{2}{h_2} p_{rt}^{(1)}, \quad F_2 = f_2 - \frac{2}{h_1} p_{zt}^{(0)} + \frac{2}{h_2} p_z^{(1)}, \quad F_3 = 0.$$

- For $(r, z) \in \gamma_{14}$

$$\Lambda_1 = -\frac{1}{r} \frac{2}{h_1} \bar{r} \bar{\sigma}_r^{(+1_z)} + \frac{1}{r} \frac{2}{h_2} \bar{r} \bar{\sigma}_{rz}^{(+1_z)} - \frac{\bar{\sigma}_\theta^{(+1_z)}}{r},$$

$$\Lambda_2 = -\frac{1}{r} \frac{2}{h_1} \bar{r} \bar{\sigma}_{rz}^{(+1_z)} + \frac{1}{r} \frac{2}{h_2} \bar{r} \bar{\sigma}_z^{(+1_z)},$$

$$\Lambda_3 = \mu, \quad F_1 = f_1 + \frac{2}{h_1} p_r^{(1)} - \frac{2}{h_2} p_{rt}^{(0)}, \quad F_2 = f_2 + \frac{2}{h_1} p_{zt}^{(1)} - \frac{2}{h_2} p_z^{(0)}, \quad F_3 = 0.$$

- For $(r, z) \in \gamma_{24}$

$$\begin{aligned}\Lambda_1 &= -\frac{1}{r} \frac{2}{h_1} \bar{r} \bar{\sigma}_r - \frac{1}{r} \frac{2}{h_2} \bar{r} \bar{\sigma}_{rz} - \frac{\bar{\sigma}_\theta}{r}, \\ \Lambda_2 &= -\frac{1}{r} \frac{2}{h_1} \bar{r} \bar{\sigma}_{rz} - \frac{1}{r} \frac{2}{h_2} \bar{r} \bar{\sigma}_z, \\ \Lambda_3 &= \mu, \quad F_1 = f_1 + \frac{2}{h_1} p_r^{(1)} + \frac{2}{h_2} p_{rt}^{(1)}, \quad F_2 = f_2 + \frac{2}{h_1} p_{zt}^{(1)} + \frac{2}{h_2} p_z^{(1)}, \quad F_3 = 0.\end{aligned}$$

The approximation of the constitutive Eqs. (3.4)–(3.6) has the following form

$$\bar{\sigma}_r = c_{33} \bar{\epsilon}_r + c_{13} (\bar{\epsilon}_\theta + \bar{\epsilon}_z) - e_{33} \bar{E}_r, \quad \bar{\sigma}_\theta = c_{13} \bar{\epsilon}_r + c_{11} \bar{\epsilon}_\theta + c_{12} \bar{\epsilon}_z - e_{13} \bar{E}_r, \quad (5.4)$$

$$\bar{\sigma}_z = c_{13} \bar{\epsilon}_r + c_{12} \bar{\epsilon}_\theta + c_{11} \bar{\epsilon}_z - e_{13} \bar{E}_r, \quad \bar{\sigma}_{rz} = c_{44} \bar{\epsilon}_{rz} - e_{15} \bar{E}_z, \quad (5.5)$$

$$\bar{D}_r = \bar{E}_r + e_{33} \bar{\epsilon}_r + e_{13} (\bar{\epsilon}_\theta + \bar{\epsilon}_z), \quad \bar{D}_z = \epsilon_{11} \bar{E}_z + 2e_{15} \bar{\epsilon}_{rz}, \quad (5.6)$$

where

$$\bar{E}_r = -\frac{1}{2} (\mu_r + \mu_r^{(-1_z)}), \quad \bar{E}_z = -\frac{1}{2} (\mu_z + \mu_z^{(-1_r)}), \quad (5.7)$$

$$\bar{\epsilon}_r = \frac{1}{2} (\delta_r^r y + \delta_r^z y^{(-1_z)}), \quad \bar{\epsilon}_\theta = \frac{1}{4\bar{r}} (y + y^{(-1_r)} + y^{(-1_z)} + y^{(-1,-1)}), \quad (5.8)$$

$$\bar{\epsilon}_z = \frac{1}{2} (\delta_z^z g + \delta_z^r g^{(-1_r)}), \quad 2\bar{\epsilon}_{rz} = \frac{1}{2} (\delta_z^r y + \delta_z^z y^{(-1_r)} + \delta_r^r g + \delta_r^z g^{(-1_z)}). \quad (5.9)$$

The approximation of the initial conditions is given as

$$y(r, z, 0) = u_r^{(0)}(r, z), \quad g(r, z, 0) = u_z^{(0)}(r, z), \quad (5.10)$$

$$\rho \delta_+^t y = \rho u_r^{(1)} + \frac{\tau}{2} (F_1 + \Lambda_1(y, g, \mu)), \quad \rho \delta_+^t g = \rho u_z^{(1)} + \frac{\tau}{2} (F_2 + \Lambda_2(y, g, \mu)). \quad (5.11)$$

Approximations (5.3)–(5.11) are of the second order accuracy in both space and time, including corners. The approximation of corners in such structures as those considered here is known to be a difficult task, and the technique for approximating corner points with the second order accuracy used here was first developed by the first author (e.g. Ref.7 and references therein).

The discrete analogue of the energy conservation law (4.2) is fundamental in investigating the system stability. One of the key steps in this investigation is to establish some bounds for the energy functional at any given moment of time. Ultimately, it is such bounds that allow us to guarantee the stability of the corresponding difference problem (5.3)–(5.11) under certain conditions on the temporal and spatial step discretizations.

6. Discrete Conservation Laws and a Generalization of the CFL Stability Condition to Coupled Problems of Piezoelectricity

The procedure described in detail for the 1D case in Ref. 6 has been generalized to the discrete model (5.3)–(5.11). In particular, by using the energy method developed for the discrete problems approximating wave dynamics (see Ref. 6 and references therein) we arrive at the following discrete analogue of the conservation law (4.2):

$$\begin{aligned} \bar{\mathcal{E}}(t + \tau) = & \bar{\mathcal{E}}(t) + 2\tau \sum_{\bar{\omega}_h} r\hbar_1\hbar_2(f_1v + f_2w) \\ & + 2\tau \left\{ \sum_{\bar{\omega}_{h_1}} [\bar{\sigma}_{rz}v + \bar{\sigma}_z w] \Big|_{Z_0}^{Z_1} + \sum_{\bar{\omega}_{h_2}} r\hbar_2[\bar{\sigma}_r v + \bar{\sigma}_{rz} w] \Big|_{R_0}^{R_1} \right\}. \end{aligned} \quad (6.1)$$

The key to our further discussion is the function $\bar{\mathcal{E}}(t)$ which represents the discrete analogue of the total energy of the electromechanical system introduced by (4.1), namely⁷

$$\begin{aligned} \bar{\mathcal{E}}(t) = & \rho \sum_{\bar{\omega}_h} r\hbar_1\hbar_2((\delta_t^- y)^2 + (\delta_t^- g)^2) + \sum_{\omega_h^+} \bar{r}\hbar_1\hbar_2 \{ c_{33}\Phi(\bar{\epsilon}_r) + c_{11}(\Phi(\bar{\epsilon}_\theta) + \Phi(\bar{\epsilon}_z)) \\ & + c_{13}[\bar{\epsilon}_r(\bar{\epsilon}_\theta + \bar{\epsilon}_z) + \bar{\epsilon}_r(\bar{\epsilon}_\theta + \bar{\epsilon}_z) - \tau^2((\delta_t^-(\bar{\epsilon}_r))((\delta_t^-(\bar{\epsilon}_\theta)) + ((\delta_t^-(\bar{\epsilon}_z)))))] \\ & + c_{12}[\bar{\epsilon}_z\bar{\epsilon}_\theta + \bar{\epsilon}_z\bar{\epsilon}_\theta - \tau^2(\delta_t^-(\bar{\epsilon}_z)(\delta_t^-(\bar{\epsilon}_\theta))] + 2c_{44}\Phi(\bar{\epsilon}_{rz}) \\ & + \epsilon_{33}\Phi(\bar{E}_r) + \epsilon_{11}\Phi(\bar{E}_z)\}, \end{aligned} \quad (6.2)$$

with

$$\Phi(y) = \frac{(y + \tilde{y})^2}{4} - \frac{\tau^2}{4}((\delta_t^- y)^2). \quad (6.3)$$

Since this function represents the energy function on the grid, it should be non-negative. The proposed scheme (5.3)–(5.11) is explicit in its essence, and therefore it is natural to expect that in order to satisfy the condition of non-negativeness certain relationships between spatial and temporal discretization steps should be fulfilled. As soon as such relationships are satisfied the following procedure can be applied to obtained an estimate of the function $\bar{\mathcal{E}}(t)$ via the initial data of the problem:

- Firstly, (6.1) is summed up over t from τ to a certain t_1 ($\tau \leq t_1 \leq T$).
- Then, all terms in the right hand side of the resulting equality are estimated by using the Sobolev embedding theorems (e.g. Refs. 10 and 28), and other discrete inequalities, such as the Friedrichs inequality connecting norms of a discrete function and its difference derivative.
- Finally, the application of the discrete analogue of Gronwall's lemma and the Cauchy–Schwartz inequality (the later is used to estimate terms of the discrete analogue of the Maxwell equation) will complete the procedure.

We omit here technical details of the numerical analysis required for such estimates. Instead, we concentrate on the requirement of non-negativeness of $\bar{\mathcal{E}}(t)$.

Firstly, we note that the first term in (6.3) is nonnegative, hence it does not require from us any extra efforts. Then, we estimate the terms associated with \bar{E}_r and \bar{E}_z from below. In particular, from the general procedure underlined above we can obtain the following result:

$$\begin{aligned} & -\epsilon_{33} \sum_{\omega_h^+} \bar{r} h_1 h_2 ((\delta_t^- (\bar{E}_r))^2 - \epsilon_{11} \sum_{\omega_h^+} \bar{r} h_1 h_2 ((\delta_t^- (\bar{E}_z))^2 \\ & \geq \frac{1}{\epsilon^M} \left[\frac{\epsilon_{33}^2}{\epsilon_{33}} \sum_{\omega_h^+} \bar{r} h_1 h_2 ((\delta_t^- (\bar{\epsilon}_r))^2 + \frac{\epsilon_{13}}{\epsilon_{33}} \sum_{\omega_h^+} \bar{r} h_1 h_2 ((\delta_t^- (\bar{\epsilon}_\theta + \bar{\epsilon}_z))^2 \right. \\ & \quad \left. + \frac{4\epsilon_{15}^2}{\epsilon_{33}} \sum_{\omega_h^+} \bar{r} h_1 h_2 ((\delta_t^- (\bar{\epsilon}_{rz}))^2 \right], \end{aligned} \quad (6.4)$$

where $\epsilon^M = \min\{1/2, \epsilon_{11}/\epsilon_{33}\}$. This estimate together with the ellipticity condition (3.7) allows us to obtain the following inequality

$$\begin{aligned} & \rho \sum_{\bar{\omega}_h} r h_1 h_2 (((\delta_t^- y)^2 + ((\delta_t^- g)^2) - \tau^2 \left(\frac{c_{33}}{4} + \frac{\epsilon_{33}^2}{4\epsilon_{33}\epsilon^M} \right) \sum_{\omega_h^+} \bar{r} h_1 h_2 ((\delta_t^- (\bar{\epsilon}_r))^2 \\ & - \tau^2 \left[\frac{c_{11}}{4} + \frac{\epsilon_{13}^2}{4\epsilon_{33}\epsilon^M} \right] \sum_{\omega_h^+} \bar{r} h_1 h_2 ((\delta_t^- (\bar{\epsilon}_\theta + \bar{\epsilon}_z))^2 - \tau^2 \left[\frac{2c_{44}}{4} + \frac{(2\epsilon_{15})^2}{4\epsilon_{33}\epsilon^M} \right] \\ & \times \sum_{\omega_h^+} \bar{r} h_1 h_2 (\delta_t^- (\bar{\epsilon}_{rz}))^2 - \frac{\tau^2}{2} c_{13} \sum_{\omega_h^+} \bar{r} h_1 h_2 \delta_t^- (\bar{\epsilon}_r) (\delta_t^- (\bar{\epsilon}_\theta) + \delta_t^- (\bar{\epsilon}_z)) \\ & - \frac{\tau^2}{2} c_{12} \times \sum_{\omega_h^+} \bar{r} h_1 h_2 \delta_t^- (\bar{\epsilon}_z) \delta_t^- (\bar{\epsilon}_\theta) \geq 0. \end{aligned} \quad (6.5)$$

In order to “extract” the stability condition from (6.5), we need to estimate the quadratic and mixed terms involving mechanical strains. This can be done in a straightforward manner if we account for the geometry of our problem. In particular, we get the following estimates

$$\begin{aligned} \sum_{\omega_h^+} \bar{r} h_1 h_2 (\bar{\epsilon}_r)^2 & \leq \frac{4}{h_1^2} \left(1 + \frac{h_1}{2R_0} \right) \sum_{\bar{\omega}_h} r h_1 h_2 y^2, \quad \sum_{\omega_h^+} \bar{r} h_1 h_2 (\bar{\epsilon}_\theta)^2 \leq \frac{1}{R_0^2} \sum_{\bar{\omega}_h} r h_1 h_2 y^2, \\ \sum_{\omega_h^+} \bar{r} h_1 h_2 (\bar{\epsilon}_z)^2 & \leq \frac{4}{h_2^2} \left(1 + \frac{h_1}{2R_0} \right) \sum_{\bar{\omega}_h} r h_1 h_2 g^2, \quad \sum_{\omega_h^+} \bar{r} h_1 h_2 \bar{\epsilon}_r \bar{\epsilon}_\theta \leq \frac{1}{2R_0 h_1} \sum_{\bar{\omega}_h} r h_1 h_2 y^2, \end{aligned}$$

$$\sum_{\omega_h^+} \bar{r} h_1 h_2 (\bar{\epsilon}_{rz})^2 \leq \frac{1}{2} \left[\frac{4}{h_2^2} \sum_{\omega_h} r \hbar_1 \hbar_2 y^2 \left(1 + \frac{h_1}{2R_0} \right) + \frac{4}{h_1^2} \sum_{\omega_h} r \hbar_1 \hbar_2 g^2 \left(1 + \frac{h_1}{2R_0} \right) \right],$$

$$\sum_{\omega_h^+} \bar{r} h_1 h_2 \bar{\epsilon}_z \bar{\epsilon}_\theta \leq \frac{1}{4R_0 h_2} \sum_{\omega_h} r \hbar_1 \hbar_2 (g^2 + y^2),$$

$$\sum_{\omega_h^+} \bar{r} h_1 h_2 \bar{\epsilon}_r \bar{\epsilon}_z \leq \frac{1}{2h_1 h_2} \sum_{\omega_h} r \hbar_1 \hbar_2 (y^2 + g^2).$$

By using these inequalities in (6.5), it is easy to see that (6.5) is satisfied if the following inequality

$$\begin{aligned} \sum_{\omega_h} r \hbar_1 \hbar_2 (\delta_t^- y)^2 & \left\{ \rho - \tau^2 \left[\frac{4}{h_1^2} \left(1 + \frac{h_1}{2R_0} \right) \left(\frac{c_{33}}{4} + \frac{e_{33}^2}{4\epsilon_{33}\epsilon^M} \right) + \frac{1}{R_0^2} \left(\frac{c_{11}}{4} + \frac{e_{13}^2}{4\epsilon_{33}\epsilon^M} \right) \right. \right. \\ & \left. \left. + \frac{4}{h_2^2} \left(1 + \frac{h_1}{2R_0} \right) \left(\frac{c_{44}}{4} + \frac{e_{15}^2}{2\epsilon_{33}\epsilon^M} \right) + c_{13} \frac{1}{4h_1 R_0} + c_{13} \frac{1}{4h_1 h_2} + c_{12} \frac{1}{8h_2 R_0} \right] \right\} \\ & + \sum_{\omega_h} r \hbar_1 \hbar_2 (g_t)^2 \left\{ \rho - \tau^2 \left[\frac{4}{h_2^2} \left(1 + \frac{h_1}{2R_0} \right) \left(\frac{c_{11}}{4} + \frac{e_{13}^2}{4\epsilon_{33}\epsilon^M} \right) \right. \right. \\ & \left. \left. + \frac{4}{h_1^2} \left(1 + \frac{h_1}{2R_0} \right) \left(\frac{c_{44}}{4} + \frac{e_{15}^2}{2\epsilon_{33}\epsilon^M} \right) + \frac{c_{13}}{4h_1 h_2} + \frac{c_{12}}{8h_2 R_0} \right] \right\} \geq \epsilon, \end{aligned} \quad (6.6)$$

holds for $\epsilon > 0$. Hence, as soon as we have

$$\begin{aligned} \rho - \epsilon_1^0 & \geq \frac{\tau^2}{h_1^2} \left[\left(1 + \frac{h_1}{2R_0} \right) \left(c_{33} + \frac{e_{33}^2}{\epsilon_{33}\epsilon^M} \right) + \frac{c_{13}}{8} \frac{h_1}{h_2} \right. \\ & \left. + \frac{c_{13}}{4R_0} h_1 + \frac{1}{4R_0^2} \times \left(c_{11} + \frac{e_{13}^2}{\epsilon_{33}\epsilon^M} \right) h_1^2 \right] \\ & + \frac{\tau^2}{h_2^2} \left[\left(1 + \frac{h_1}{2R_0} \right) \left(c_{44} + \frac{2e_{15}^2}{\epsilon_{33}\epsilon^M} \right) + \frac{c_{12}}{8R_0} h_2 + \frac{c_{13}}{8} \frac{h_2}{h_1} \right], \end{aligned} \quad (6.7)$$

$$\begin{aligned} \rho - \epsilon_2^0 & \geq \frac{\tau^2}{h_2^2} \left[\left(1 + \frac{h_1}{2R_0} \right) \left(c_{11} + \frac{e_{13}^2}{\epsilon_{33}\epsilon^M} \right) + \frac{c_{12}}{8R_0} h_2 + \frac{c_{13}}{8} \frac{h_2}{h_1} \right] \\ & + \frac{\tau^2}{h_1^2} \left[\left(1 + \frac{h_1}{2R_0} \right) \left(c_{44} + \frac{2e_{15}^2}{\epsilon_{33}\epsilon^M} \right) + \frac{c_{13}}{8} \frac{h_1}{h_2} \right], \end{aligned} \quad (6.8)$$

for $\epsilon_i^0 > 0$, $i = 1, 2$, the nonnegativeness of the discrete energy function is guaranteed.

We know (e.g. Refs. 17 and 29) that in the general case of anisotropic electro-elastic media there are three plane waves, namely quasi-longitudinal and two quasi-transverse (the latter usually propagate slower than the quasi-longitudinal

one). Hence, in order to explain (6.7)–(6.8) from a physical point of view, we introduce three quantities

$$c_1 = \sqrt{\frac{c_{33}(1+K_1)}{\rho}}, \quad c_2 = \sqrt{\frac{c_{44}(1+K_2)}{\rho}}, \quad c_3 = \sqrt{\frac{c_{11}(1+K_3)}{\rho}}, \quad (6.9)$$

characterizing the velocities of these three waves. In (6.9),

$$K_1 = \frac{e_{33}^2}{\epsilon_{33}c_{33}}, \quad K_2 = \frac{e_{15}^2}{\epsilon_{11}c_{44}}, \quad K_3 = \frac{e_{13}^2}{\epsilon_{11}c_{11}}, \quad (6.10)$$

are constants of electromechanical coupling. Therefore, from (6.7)–(6.8), we deduce the stability conditions for the numerical approximations (5.3)–(5.11)

$$\begin{aligned} & \frac{\tau^2}{h_1^2} c_1^2 \left[\left(1 + \frac{h_1}{2R_0}\right) A_0^1 + A_1^1 \frac{h_1}{h_2} + A_2^1 h_1 + A_3^1 h_1^2 \right] \\ & + \frac{\tau^2}{h_2^2} c_2^2 \left[\left(1 + \frac{h_1}{2R_0}\right) \times B_0^1 + B_1^1 \frac{h_2}{h_1} + B_2^1 h_2 \right] \leq 1 - \epsilon_1, \end{aligned} \quad (6.11)$$

$$\begin{aligned} & \frac{\tau^2}{h_2^2} c_3^2 \left[\left(1 + \frac{h_1}{2R_0}\right) B_0^2 + B_1^2 \frac{h_2}{h_1} + B_2^2 h_2 \right] \\ & + \frac{\tau^2}{h_1^2} c_2^2 \left[\left(1 + \frac{h_1}{2R_0}\right) A_0^2 + A_1^2 \frac{h_1}{h_2} \right] \leq 1 - \epsilon_2, \end{aligned} \quad (6.12)$$

where $\epsilon, \epsilon_i, \epsilon_i^0, i = 1, 2$ are positive constants that do not depend on step discretizations τ, h_1 and h_2 , and all electromechanical constants are given explicitly by

$$\begin{aligned} A_0^1 &= \frac{1 + K_1/\epsilon^M}{1 + K_1}, \quad A_1^1 = \frac{c_{13}}{8c_{33}(1+K_1)}, \quad A_2^1 = \frac{c_{13}}{4R_0c_{33}(1+K_1)}, \\ A_3^1 &= \frac{(c_{11} + e_{13}^2/(\epsilon_{33}\epsilon^M))}{4R_0^2c_{33}(1+K_1)}, \quad B_0^1 = \frac{1 + 2K_2/\epsilon^M}{1 + K_2}, \quad B_1^1 = \frac{c_{13}}{8c_{44}(1+K_2)}, \\ B_2^1 &= \frac{c_{12}}{8R_0c_{44}(1+K_2)}, \quad B_0^2 = \frac{1 + K_3/\epsilon^M}{1 + K_3}, \quad B_1^2 = \frac{c_{13}}{8c_{11}(1+K_3)}, \\ B_2^2 &= \frac{c_{12}h_2}{8R_0c_{11}(1+K_1)}, \quad A_0^2 = \frac{1 + 2K_2/\epsilon^M}{1 + K_2}, \quad A_1^2 = \frac{c_{13}}{8c_{44}(1+K_2)}, \end{aligned}$$

and can be evaluated immediately for each specific material and the given geometry.

Conditions (6.11)–(6.12) provide a generalization of the Courant–Friedrichs–Lewy stability condition to the case of coupled dynamic piezoelectricity, and link together discretization steps τ, h_1 and h_2 with the velocity of mixed electro-elastic waves. Several interesting corollaries follow from (6.11)–(6.12) as special cases. In particular, in the case of isotropic solid in the absence of electric field¹⁷ $c_{11} = c_{33} = \tilde{\lambda} + 2\tilde{\mu}$, $c_{12} = c_{13} = \tilde{\lambda}$, $c_{44} = \tilde{\mu}$, and $K_1 = K_2 = K_3 = 0$, where $\tilde{\lambda}$ and $\tilde{\mu}$ are the

Lame coefficients. In this case, the stability conditions (6.11)–(6.12) are reduced to the following conditions (written here in their principal parts)

$$\frac{\tau^2}{h_1^2} \left(\tilde{\lambda} + 2\tilde{\mu} + \frac{\tilde{\lambda}}{8} - \frac{h_1}{h_2} \right) + \frac{\tau^2}{h_2^2} \left(\tilde{\mu} + \frac{\tilde{\lambda}}{8} - \frac{h_2}{h_1} \right) \leq 1 - \epsilon_1, \quad (6.13)$$

$$\frac{\tau^2}{h_2^2} \left(\tilde{\lambda} + 2\tilde{\mu} + \frac{\tilde{\lambda}}{8} - \frac{h_2}{h_1} \right) + \frac{\tau^2}{h_1^2} \left(\tilde{\mu} + \frac{\tilde{\lambda}}{8} - \frac{h_1}{h_2} \right) \leq 1 - \epsilon_2. \quad (6.14)$$

It is easy to see, by summing (6.13) and (6.14) up and taking into account that $\frac{\tau^2}{h_1 h_2} \leq \frac{1}{2}(\frac{\tau^2}{h_1^2} + \frac{\tau^2}{h_2^2})$, that the stability condition typical for pure elastic problems (e.g. Ref. 30) is a special case of (6.11) and (6.12).

7. Computational Examples and Concluding Remarks

In this section we present some typical examples resulting from computations of vibrational characteristics of finite piezoelectric cylinders made of PZT-piezoceramics and polarized preliminary radially and circularly. The choice of PZT materials is natural not only due to a low cost and relatively easy process of fabrication of PZT-based geometric configurations such as cylindrical shells, but also due to other advantages this material offers, including its resistance to mechanical and electrical stress-induced depolarization and a moderate operating temperature range. Large piezoelectric coefficients of PZT-ceramics allow the extensive use of these materials in industrial applications. Our interest in hollow piezoceramic structures is inspired by the existing and potential applications of miniaturized piezoceramic transducers in acoustics, biomedical imaging, sensor and hydrophone design, consumer electronics and other areas.^{31,32} Hollow piezoelectric cylinders provide a natural framework for studying electromechanical wave propagation in bone tissues (e.g. Refs. 33 and 34). And, of course, many challenges of modeling piezoceramic structures during recent years have also been provided by “smart” properties of materials, reflecting a resemblance in the behaviour of some piezoceramic materials to the behaviour of biological systems. For example, the mechanism by which fishes sense vibrations can be mimicked by piezoelectric hydrophones. Some piezoelectric materials are able to “remember” their original shape whereas others can even “learn” as environmental properties change (see Ref. 35 and references therein).

Since most computational results reported in the literature are pertinent to the case of axial preliminary polarization our results might be used for further comparisons of technical characteristics of piezoelectric devices manufactured under different preliminary polarization conditions. The results on infinite length hollow cylinders have been already reported in the literature (e.g. Refs. 5 and 6 and references therein), and some results in the two-dimensional case have been also presented (e.g. Ref. 7). Note that our numerical procedure can be applied to practically arbitrary electromechanical loading conditions in the general dynamic

situations, while a vast majority of the results available in the literature up to date is limited to the harmonic oscillation case only.

The results presented here are for hollow cylinders of length 1 in dimensionless units and thickness 0.2 and 0.05. The time dependency of radial displacements on the external surface of cylinders is presented in Fig. 2. Compared to the infinite-length cylinder case discussed earlier (e.g. Ref. 5), we observe a noticeable decrease in the magnitude of displacements for cylinders polarized radially. In contrast to that, we observe a certain increase in the magnitude of displacements for finite-length cylinders poled circularly, although such an increase is not quantitatively essential. Radial and axial components of displacements at a fixed moment in time, $t = 10$, in finite-length cylinders poled radially are shown in Fig. 3. Despite relatively small number of spatial discretization points chosen in this example, the symmetry pattern is clearly observed with the level curves. Such a symmetry pattern is preserved not only for displacements presented here, but also for stresses. From a quantitative point of view it is also seen that a strong electromechanical coupling in the case of the radial preliminary polarization leads to a larger magnitude in vibrations compared to the case of the circular preliminary polarization.

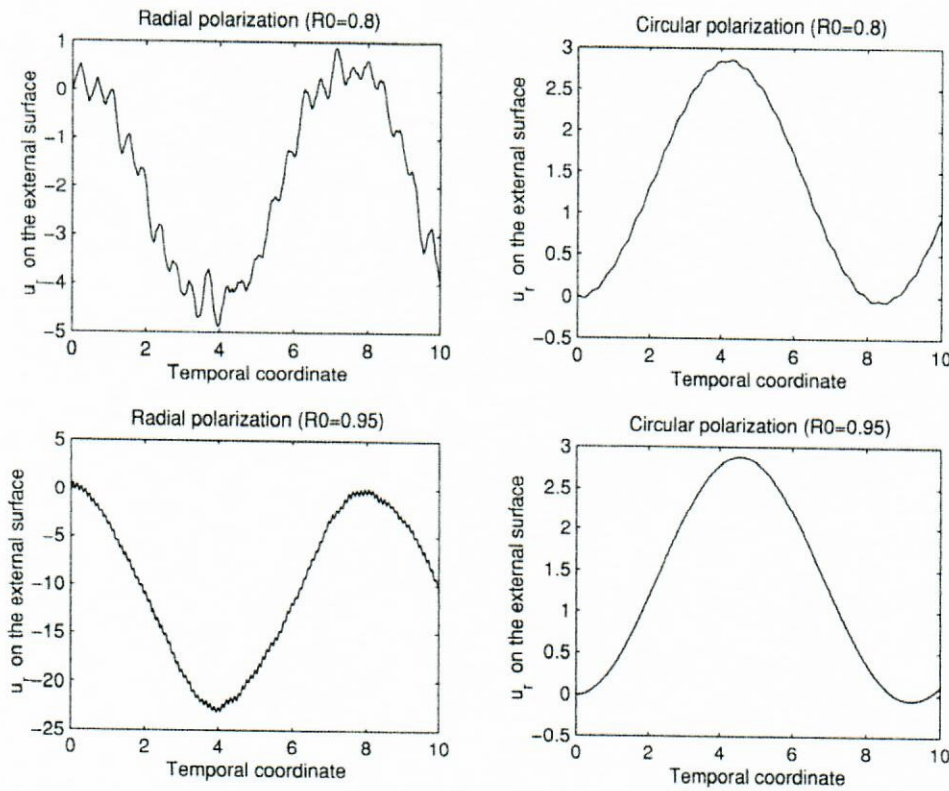
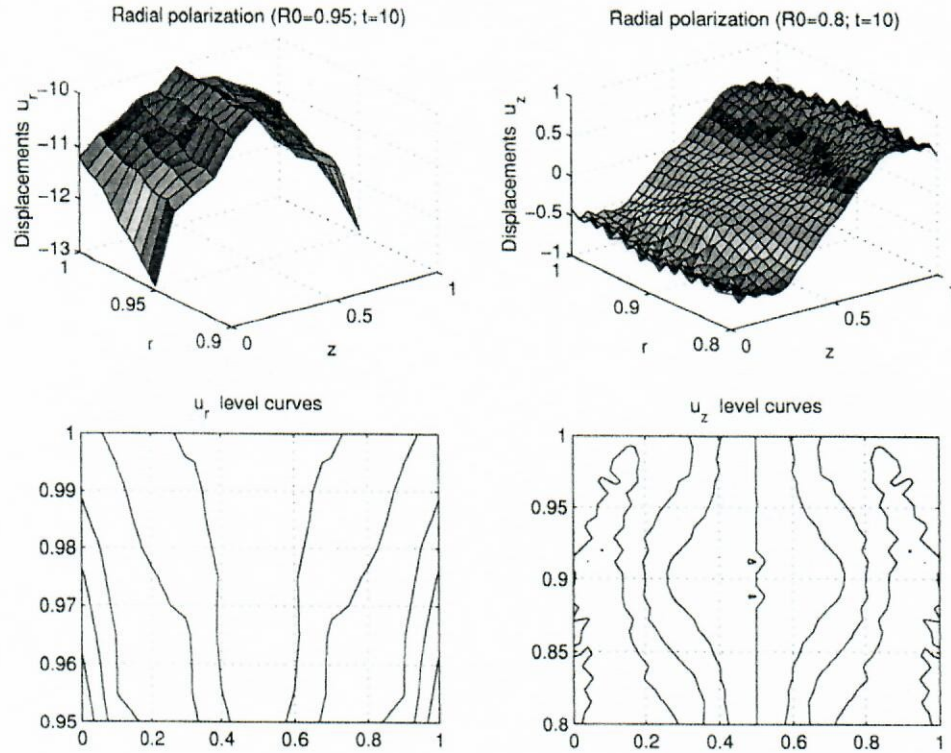


Fig. 2. Dynamics of radial displacements on the external surface.

Fig. 3. Radial and axial displacements at $t = 10$.

The problems considered in this paper belong to the domain of coupled field theory,^{5,6,8,15,36}, and they are often termed as multiphysics problems. For all such problems the role of the physical parameterization of mathematical models will continue to increase allowing to incorporate new, more precise information as a result of measurements and experiments. On the other hand, the construction of the numerical grid for the problem solution is contingent on the property of the solution which is sought on that grid, the fact which inevitably leads to the use of some *a priori* information about the solution properties. Hence, being an integral part of the model construction, the physical parameterization may decisively influence the complexity of numerical algorithms. Under such circumstances the importance of computationally efficient explicit numerical approximations increases, and the investigation of the stability of discrete models becomes the main issue in the success of the whole modelling enterprise. The methodology discussed in this paper provides a general framework to not only constructing efficient explicit numerical approximations for coupled problems of piezoelectricity but also to deriving stability conditions for such approximations based on the energy method and discrete conservation laws.

References

1. Y. Kagawa, T. Tsuchiya and T. Kawashima, "FE simulation of piezoelectric vibrator gyroscopes," *IEEE Trans. Ultrason. Ferroelectr. Freq. Contr.* **43**(4), pp. 509–120, 1996.
2. J. S. Lee, "Boundary element method for electroelastic interaction in piezoceramics," *Eng. Anal. Boundary Elem.* **15**(4), pp. 321–328, 1995.
3. P. Lu and O. Mahrenholtz, "A variational boundary element formulation for piezoelectricity," *Mech. Rés. Commun.* **21**(6), pp. 605–615, 1994.
4. R. V. N. Melnik and K. N. Melnik, "A note on the class of weakly coupled problems of non-stationary piezoelectricity," *Commun. Numer. Meth. Eng.* **14**, pp. 839–847, 1998.
5. R. V. N. Melnik, "The stability condition and energy estimate for non-stationary problems of coupled electroelasticity," *Math. Mech. Solids* **2**(2), pp. 153–180, 1997.
6. R. V. N. Melnik, "Convergence of the operator-difference scheme to generalized solutions of a coupled field theory problem," *J. Diff. Eq. Appl.* **4**, pp. 185–212, 1998.
7. R. V. N. Melnik, "Generalised solutions, discrete models and energy estimates for a 2D problem of coupled field theory," *Appl. Math. Comput.* **107**, pp. 27–55, 2000.
8. R. V. N. Melnik, "Numerical analysis of dynamic characteristics of coupled piezoelectric systems in acoustic media," *Math. Comput. Sim.*, Elsevier, to appear, 2002.
9. R. Courant, K. Friedrichs and H. Lewy, "On partial differential equations of mathematical physics," Technical Report NYO-7689, AEC Computing Facility, Institute of Mathematical Sciences, New York University, September (English translation of the paper originally published in Volume 100 of *Mathematische Annalen*, 1928), pp. 1–76, 1956.
10. A. A. Samarskii, *The Theory of Difference Schemes*, Marcel Dekker, New York, 2001.
11. Y. Bao, H. S. Tzou and V. B. Venkayya, "Analysis of non-linear piezothermoelastic laminated beams with electric and temperature effects," *J. Sound Vibration* **209**(3), pp. 505–518, 1998.
12. Y. Ootao and Y. Tanigawa, "Three-dimensional transient piezothermoelasticity in functionally graded rectangular plate bonded to a piezoelectric plate," *Int. J. Solids Struct.* **37**, pp. 4377–4401, 2000.
13. R. Ye and H. S. Tzou, "Control of adaptive shells with thermal and mechanical excitations," *J. Sound Vibration*, **231**(5), pp. 1321–1338, 2000.
14. W. Q. Chen, "Vibration theory of non-homogeneous spherically isotropic piezoelastic bodies," *J. Sound Vibration* **236**(5), pp. 833–860, 2000.
15. R. V. N. Melnik, "Computational analysis of coupled physical fields in piezothermoelastic media," *Comput. Phys. Commun.* **142**(1–3), pp. 231–237, 2001.
16. T. Ikeda, *Fundamentals of Piezoelectricity*, Oxford University Press, Oxford, 1990.
17. D. Royer and E. Dieulesaint, *Elastic Waves in Solids*, 2 Vols., Springer, 2000.
18. S. S. Antman, *Nonlinear Problems of Elasticity*, Springer, 1995.
19. H. Li *et al.*, "Free vibration of piezoelectric laminated cylindrical shells under hydrostatic pressure," *Int. J. Solids Struct.* **38**, pp. 7571–7585, 2001.
20. J. L. Rose, *Ultrasonic Waves in Solid Media*, Cambridge University Press, 1999.
21. N. N. Rogacheva, "The dependence of the electromechanical coupling coefficient of piezoelectric elements on the position and size of the electrodes," *PMM J. Appl. Math. Mech.* **65**(2), pp. 317–326, 2001.
22. W. Voigt, *Lehrbuch der Kristall-Physik*, Leipzig, Teubner, 1910.
23. R. V. N. Melnik, "Existence and uniqueness theorems of the generalised solutions for a class of non-stationary problems of coupled electroelasticity," *Sov. Math. (Iz. VUZ)*, **35**(4), pp. 24–32, 1991.

24. D. Furihata, "Finite difference schemes for $\frac{\partial u}{\partial t} = (\frac{\partial}{\partial x})^\alpha \frac{\delta G}{\delta u}$ that inherit energy conservation or dissipation property," *J. Comput. Phys.* **156**, pp. 181–205, 1999.
25. M. Shashkov and S. Steinberg, *Conservative Finite Difference Methods on General Grids*, CRC Press, Boca Raton, 1995.
26. R. V. N. Melnik and I. P. Gavrilyuk, "Computationally efficient parallel algorithms for time-dependent convection-diffusion models," *Proc. Fifth World Cong. Comput. Mech.*, eds. H. A. Mang, F.G. Rammerstorfer and J. Eberhardsteiner, pp. 1–10, 2002.
27. V. Dorodnitsyn and P. Winternitz, "Lie point symmetry preserving discretizations for variable coefficient Kortweg-de Vries equations", *Nonlin. Dynam.* **22**, pp. 49–59, 2000.
28. A. A. Samarskii and E. S. Nikolaev, *Numerical Methods for Grid Equations*, Birkhauser Verlag, Basel, Boston, 1989.
29. D. A. Berlincourt, D. R. Curran and H. Jaffe, "Piezoelectric and piezomagnetic materials and their function in transducers," *Phys. Acoustics*, Vol. 1A, ed. W. P. Mason, New York and London: Academic Press, pp. 204–236, 1964.
30. M. N. Moskalkov and D. Utebaev, "On the convergence of centered difference schemes for dynamic problems of elasticity theory," *Diff. Eq.* **21**(7), pp. 1238–1246, 1985.
31. J. T. Fielding *et al.*, "Characterization of PZT hollow-sphere transducers," *Proc. IX IEEE Int. Symp. Appl. Ferroelec.* pp. 202–205, 1994.
32. R. Meyer, Jr. *et al.*, "Lead zirconate titanate hollow-sphere transducers," *J. Am. Cer. Soc.* **77**, pp. 1669–1672, 1994.
33. A. M. El-Naggar, A. M. Abd-Alla and S. R. Mahmoud, "Analytical solution of electro-mechanical wave propagation in long bones," *Appl. Math. Comput.* **119**, pp. 77–98, 2001.
34. D. I. Fotiadis, G. Foutsitzi and C. V. Massalas, "Wave propagation modeling in human long bones," *Acta Mech.* **137**, pp. 65–81, 1999.
35. R. E. Newnham and K. A. Markowski, "Composite transducer and actuators," *Proc. IX IEEE Int. Symp. Appl. Ferroelec.* pp. 705–708, 1994.
36. R. V. N. Melnik, "Discrete models of coupled dynamic thermoelasticity for stress-temperature formulations," *Appl. Math. Comput.* **122**, pp. 107–132, 2001.